A Slip Model for the Spherical Actuation of the Atlas Motion Platform

J.B. HOLLAND, M.J.D. HAYES, and R.G. LANGLOIS
Department of Mechanical & Aerospace Engineering, Carleton University,
1125 Colonel By Drive, Ottawa, ON, K1S 5B6, Canada,
j.holland@telesat.ca, jhayes@mae.carleton.ca, rlangloi@mae.carleton.ca

Abstract

The Atlas platform represents a novel six degree-of-freedom motion platform architecture. Orienting is decoupled from positioning, and unlimited rotations are possible about every axis. The decoupling is accomplished by fixing a three degree-of-freedom spherical orienting device, called the Atlas sphere, on a gantry with three orthogonal linear axes. The key to the design is three omni-directional wheels in an equilateral arrangement, which impart angular displacement to a sphere, providing rotational actuation. The free-spinning castor rollers provide virtually friction-free motion parallel to each omni-wheel rotation axis creating the potential for unconstrained angular motion. Since the sphere directly contacts the omni-wheels, there are no joints or links interfering with its motion, allowing full 360° motion about all axes. However, the kinematic constraints are non-holonomic. This paper explores the slip at the interface between each omni-wheel and the Atlas sphere. A kinematic slip model is presented, introducing the *slip ratio* (ratio of each omni-wheel tangential velocity at the interface to that of the sphere at the same point). The long-term goal is to incorporate the slip model into a control law for position level control of the sphere. Two illustrative examples are given.

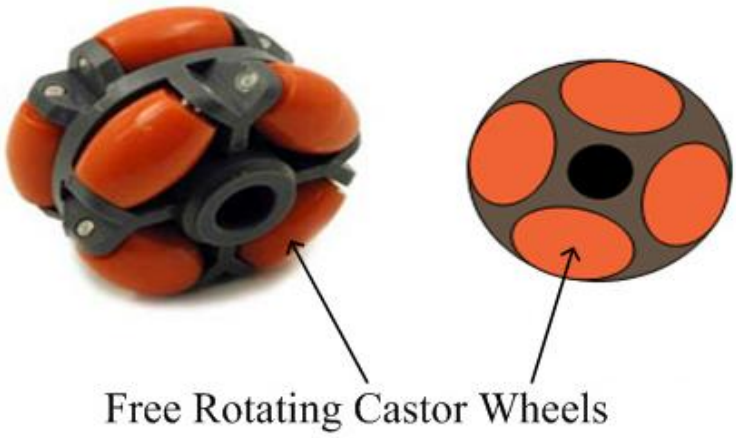

Figure 1: An *omni-directional*, or *omni-wheel*.

1 Introduction

The Atlas platform is a novel conceptual design resulting from the Carleton University Simulator Project (CUSP). CUSP is one of six multidisciplinary capstone 4th year design projects offered by the Department of Mechanical and Aerospace Engineering at Carleton. It is currently in its third annual phase. The initial goal of CUSP was to design a motion platform where positioning and orienting were decoupled. This was easily proposed by mounting a spherical mechanism on a gantry platform with three linear axes. The major design challenge was obtaining unlimited rotations about any axis. The concept of Atlas employs *Mekanum omni-directional wheels* [1], now popularly known as *omni-wheels*, as actuators driving the motion of a centred spherical device (Atlas sphere) situated on the omni-wheels.

Omni-wheels (see Figure 1) are similar to normal frictional wheels but consist of a number of free spinning castor wheels positioned on the periphery of the wheel circumference allowing for near-friction-free movement parallel to the onmi-wheels's axes of rotation. These omni-wheels are the key to unrestricted angular motion of the Atlas sphere. Utilizing three omni-wheels rigidly mounted in a triangulated arrangement, the Atlas sphere rests on the omni-wheels which are controlled independently. Linear combinations of the three omni-wheel angular velocities generate rotational motion of the Atlas sphere through any angle about any axis (see Figure 2).

Of course, the concept of a spherical actuator is not new. For example spherical dc induction motors were introduced in 1959 by Williams, et al. in [2]. Developments continued over the next 30 years leading to designs presented in [3, 4, 5]. However, due to physical limitations imposed by the stator and commutator, angular displacements are limited. The ability to produce continuous unlimited angular displacements in roll, pitch and yaw puts Atlas in new territory in terms of freedom of motion in mechanical devices thereby making it desireable for applications ranging from vehicle simulator motion platforms, to satellite attitude acquisition device calibration, to gaming applications.

As the Atlas sphere is driven by the three omni-wheels, the angular velocity of the sphere is proportional to a linear combination of the angular velocities, less the free spinning across the castors on the periphery of each omni-wheel, less the slip and scrub on the castors. In most

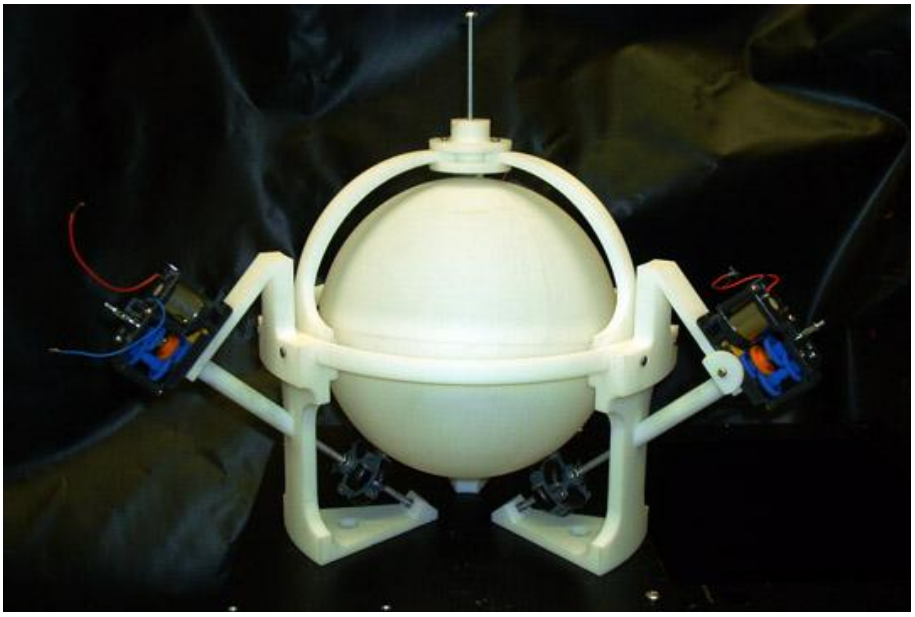

Figure 2: Atlas proof-of-concept demonstrator.

cases the sphere's tangential velocity at the contact point of each omni-wheel and that of the corresponding point on the omni-wheel itself will be different. This will produce slip at the three contact points as well as scrub. For clarity in the context of this paper, *slip* refers to differences in translational velocity whereas *scrub* refers to differences in angular velocity between contacting bodies. The focus of this paper is limited to slip. Spherical platform velocity-level kinematics and the associated Jacobian matrix relating omni-wheel angular velocities to the angular velocity of the Atlas sphere, developed in [6], are used to investigate the slip behaviour of the Atlas sphere on the omni-wheels.

2 Atlas Platform Description

The Atlas platform is a novel conceptual design that allows unlimited angular displacements about any (every) axis through the geometric centre of the sphere. It is essentially an inverted mouse-ball. A conventional roller-ball mouse uses two orthogonally-mounted sensors to follow the motion of the ball contact point on the plane of the mouse-pad. In the case of Atlas, the sphere is driven by three omni-wheels. This in turn is an adaptation of three-omni-wheeled vehicles that move in the plane [7]. Any angular velocity about any central sphere axis can be generated by linear combinations of angular velocities of the three omni-wheels. Omni-wheels have free moving castor wheels along their periphery [8]. Because the castors are free-spinning, they allow the sphere to spin in directions perpendicular to the rotation axes of the castor wheels. The omni-wheels thereby enable an unlimited rotational capability for the Atlas sphere allowing for 360° displacements in roll (about the X-axis), pitch (about the Y-axis), and yaw (about the Z-axis), as well as any linear combination. The right-handed $[X, Y, Z]$ coordinate system is identified in Figure 3.

The general kinematic architecture of the Atlas simulator motion platform consists of three

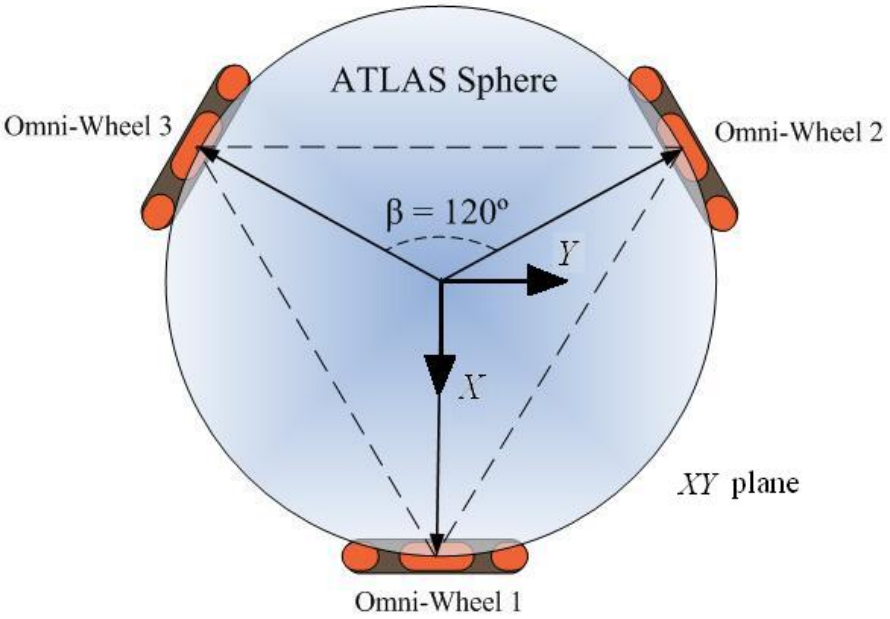

Figure 3: Omni-wheel axes projected in the XY-plane.

omni-directional wheels with each of the driving axes separated by 120° in the XY-plane, as illustrated in Figure 3. This angle is denoted β. The projection of these axes in the XY-plane forms an equilateral triangle and creates equal distribution of static weight of the sphere on each omni-wheel. Note, the omni-wheel angle relative to the XY-plane is different than that illustrated in the figure. Each omni-wheel driving axis is sloped downward by 40°, denoted α, relative to the horizontal XY-plane. This is indicated in Figures 4 and 5.

The three omni-wheels are independently actuated with variable speed DC motors allowing for each wheel to rotate at a different speed from the others. It should be noted that with the configuration of omni-wheel locations described, multiple motors contribute to sphere actuation thereby limiting individual motor torque requirements. Each omni-wheel transfers energy through friction to the Atlas sphere and contributes to the sphere's rotational velocity. Depending on the rotational speeds of each omni-wheel (and other factors such as weight, and contact surfaces not studied in this paper) the Atlas sphere will rotate at a certain angular velocity. Each roll, pitch, and yaw component of the three omni-wheels will combine and contribute to the overall angular velocity of the Atlas sphere.

For the kinematic analysis of the Atlas platform [6] seven reference coordinate frames were needed. The first being the inertial frame $[X, Y, Z]$ which is centred in the middle of the omni-wheel triangle. The inertial frame ($[X, Y, Z]$) has its X-axis pointing to omni-wheel 1, and its Z-axis perpendicular to the contact point plane which will now be designated the XY-plane, see Figure 3.

The origins of the next three reference frames are on the centre of each omni-wheel. The x-axis points outwards from the wheel centre and the z-axis points towards the contact point between the omni-wheel and Atlas sphere, illustrated in Figure 4. Each omni-wheel frame will be designated $[x_k,y_k,z_k]$ where $k \in \{1, 2, 3\}$, indicating each omni-wheel; for instance, the frame of omni-wheel

two will be designated [x_2,y_2,z_2]. The remaining three reference frames originate, one each, at each omni-wheel contact point with the sphere, but are not rotated by the tilt of the omni-wheel; this will allow for easier analysis when studying the slip factors existing at the contact points. These frames are the omni-wheel slip frames and designated [i_k,j_k,k_k], again where k indicates the wheel being considered.

The actual dimensions of the omni-wheel angular separation are dependent on the diameter of the Atlas sphere and how high the centre of the sphere will be relative to the XY-plane. The centre of the sphere can be located anywhere relative to the XY-plane. The optimal location of the Atlas sphere's centre will not be discussed in this paper and will be left as a variable. The radius vector of the Atlas sphere is the position vector of each omni-wheel contact point, expressed in $[X, Y, Z]$ as $\mathbf{R}_k$, having components $[R_{k_X}, R_{k_Y}, R_{k_Z}]$, with k indicating a particular omni-wheel, see Figure 5. Since the omni-wheel contact points are the vertices of an equilateral triangle, the norm of each radius vector is the same:

$$\|\mathbf{R}_1\| = \|\mathbf{R}_2\| = \|\mathbf{R}_3\| = \|\mathbf{R}\|. \tag{1}$$

The angle θ varies with the ratio of R_{k_Z} and R_{k_X}:

$$\theta \quad = \quad \text{atan2}\left(\frac{R_{k_Z}}{R_{k_X}}\right). \tag{2}$$

Since $\mathbf{R}_1$ is situated along the X-axis there is no R_{1_Y} component, only R_{1_X} and R_{1_Z}. The $\mathbf{R}_1$ vector points from the centre of the Atlas sphere towards the contact point of omni-wheel 1 so R_{1_X} is always positive while R_{1_Z} is always negative. As stated earlier, R_{1_X} and R_{1_Z} are left as variables for the user to define, as the optimal locations for the contact points relative to the sphere is not an issue addressed in this paper. To determine the radial vectors $\mathbf{R}_2$ and $\mathbf{R}_3$, vector $\mathbf{R}_1$ can be transformed using rotation matrices defined by the geometry of the Atlas sphere configuration illustrated in Figure 5. These transformations were also used in determining the orienting Jacobian and for characterizing sphere slip on the omni-wheels of the Atlas platform.

Two angles must be considered when calculating these transformations, α and β. The angle α is the tilt of the omni-wheel about the omni-wheel y-axis. For the current configuration, $\alpha = 40°$ for each wheel, with counter-clockwise rotations being positive. The angle β represents the rotation of each omni-wheel axis about the Z-axis, relative to the axis of omni-wheel 1. Thus $\beta_1 = 0°$, $\beta_2 = 120°$, and $\beta_3 = 240°$.

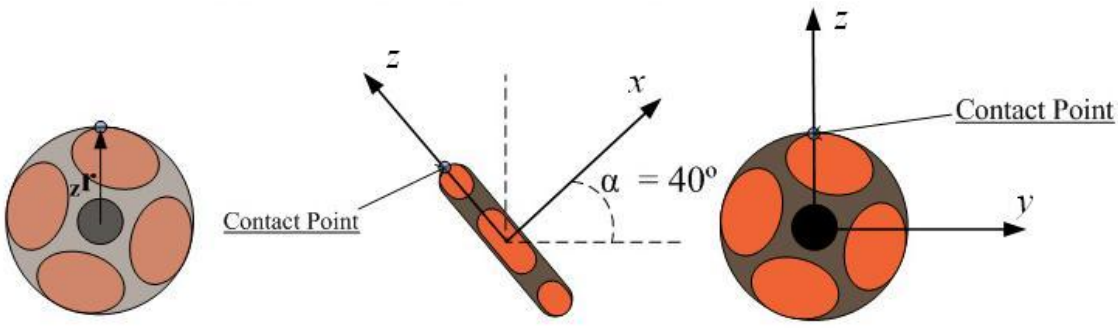

Figure 4: Omni-wheel coordinate reference frames.

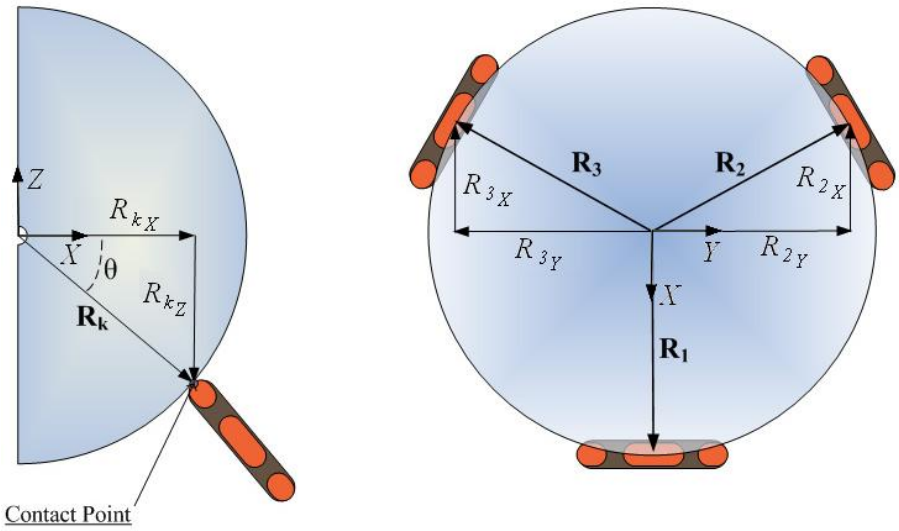

Figure 5: Sphere contact point radial vector components.

3 Relevant Kinematics

Velocity-level kinematics corresponding to the Atlas motion system, as developed by Robinson et al [6], required for developing the slip model is reproduced here. Readers are referred to the original paper for the complete derivation.

The Atlas sphere kinematics were developed based on two angular velocity vectors, $\boldsymbol{\Omega}$, and $\boldsymbol{\omega}_k$. The angular velocity of the sphere expressed in the global-frame $[X, Y, Z]$ is denoted $\boldsymbol{\Omega}$, while and the collection of three omni-wheel angular velocities about their shaft axes expressed in the omni-wheel coordinate frames $[x_k, y_k, z_k]$ is denoted $\boldsymbol{\omega}_k$, $k \in \{1, 2, 3\}$.

The tangential velocities at the respective sphere contact points lie along the k^{th} omni-wheel local y-axes and are denoted

$$\mathbf{v}_k \;=\; [0, v_{k_y}, 0]^T \;=\; \boldsymbol{\omega}_k \times \mathbf{r}_k, \tag{3}$$

where $\boldsymbol{\omega}_k$ and $\mathbf{r}_k$ are the k^{th} omni-wheel angular velocity and radial vectors (directed from the omni-wheel centre to the sphere contact point). These velocity vectors are are mapped from their respective omni-wheel coordinate frames $[x_k, y_k, z_k]$ to the global frame $[X, Y, Z]$ using geometric transformations having the form:

$$\mathbf{T}_k \;=\; \begin{bmatrix} \mathrm{c}_{\beta_k} & \mathrm{s}_{\beta_k} & 0 \\ -\mathrm{s}_{\beta_k} & \mathrm{c}_{\beta_k} & 0 \\ 0 & 0 & 1 \end{bmatrix}, \tag{4}$$

where c_{β_k}, and s_{β_k} respectively denote $\cos\beta_k$ and $\sin\beta_k$; it is possible to express the tangential velocities $\mathbf{V}_k$ at the contact points in the inertial frame:

$$\mathbf{V}_1 \;=\; [0 \;\; -\omega_1 r_z \;\; 0]^T, \tag{5}$$

$$\mathbf{V}_2 \;=\; [-\omega_2 r_z \mathrm{s}_{\beta_2} \;\; -\omega_2 r_z \mathrm{c}_{\beta_2} \;\; 0]^T, \tag{6}$$

$$\mathbf{V}_3 \;=\; [-\omega_3 r_z \mathrm{s}_{\beta_3} \;\; -\omega_3 r_z \mathrm{c}_{\beta_3} \;\; 0]^T. \tag{7}$$

Further derivation results in the relationship between omni-wheel angular velocities, $\boldsymbol{\omega}$, and the sphere angular velocity, $\boldsymbol{\Omega}$, that reveals the system Jacobian matrix $\mathbf{J}$

$$\boldsymbol{\Omega} \;=\; \mathbf{J}\boldsymbol{\omega} \;=\; \frac{r_z}{\|\mathbf{R}\|^2}\begin{bmatrix} R_{1_Z} & R_{1_Z}\mathrm{c}_{\beta_2} & R_{1_Z}\mathrm{c}_{\beta_3} \\ 0 & -R_{1_Z}\mathrm{s}_{\beta_2} & -R_{1_Z}\mathrm{s}_{\beta_3} \\ -R_{1_X} & -R_{1_X} & -R_{1_X} \end{bmatrix}\begin{bmatrix} \omega_1 \\ \omega_2 \\ \omega_3 \end{bmatrix}. \tag{8}$$

4 Slip

Because of the kinematic geometry of the sphere driven by three omni-wheels, there will typically be some slip at the contact points between the sphere and omni-wheels. Slip occurs when two contacting surfaces move such that the linear velocity at the contact point is different for each surface. Slip can be quantified in two ways: slip velocity; and slip percentage (or slip ratio). Slip is therefore a relative term. Analyzing the slip factors of the Atlas spherical platform is necessary because almost all cases of angular displacement will cause varying velocities between mating surfaces at their contact points.

To characterize the slip factors of the Atlas platform the linear tangential velocities are used. The slip factors are expressed relative to the Atlas sphere. There are two slip velocity components to be determined: the transverse velocity, $S_{\perp_k}$, and the tangential velocity, $S_{\tan_k}$. These two velocity vectors fall on the tangent plane at each contact point of the sphere and the omni-wheel, see Figure 6, and are mutually perpendicular. The transverse velocity component, $S_{\perp_k}$, is perpendicular to the free-spinning castor wheel axis. Whereas, the tangential velocity component, $S_{\tan_k}$, is perpendicular to the omni-wheel driving axis, parallel to the tangential velocity vector, $\mathbf{V}_k$. Both $S_{\perp_k}$ and $S_{\tan_k}$ lie in the omni-wheel-sphere tangent plane. The tangential velocity of slip, $S_{\tan_k}$ lies along the j-axis of the omni-wheel slip frame, illustrated in Figure 6. The transverse velocity component of slip, $S_{\perp_k}$, lies along the tangential plane of the contact point and the Atlas sphere, which is θ° relative to the k-axis. The tangent plane, which is perpendicular to both the contact point and $\mathbf{R}_k$, can be determined using the angle θ from Equation (2). This indicates that the tangential plane varies with the radius of the Atlas sphere and location of the contact points relative to the XY-plane.

The velocities in the tangential and transverse direction must be found for both the omni-wheels and the Atlas sphere at the contact points. The omni-wheel's tangential-velocities are expressed in the omni-wheel slip frame by Equation (3), and in the inertial frame by Equations (5-7). The transverse-velocity of the omni-wheel is 0; this is because there is no actuation of the wheel in that direction. The transverse-velocity of the Atlas sphere at each contact point is therefore unconstrained by the omni-wheel because the castor wheels on the periphery of each omni-wheel are free spinning. The tangential and transverse slip velocity components of the Atlas sphere must be calculated separately.

To compute the sphere linear velocities at the omni-wheel contact points, $\boldsymbol{\Lambda}_k$, $k \in \{1,2,3\}$, we use the cross-product of the angular velocity of the Atlas sphere, $\boldsymbol{\Omega}$, and the three radial vectors $\mathbf{R}_k$:

$$\boldsymbol{\Lambda}_k \;=\; \boldsymbol{\Omega} \times \mathbf{R}_k. \tag{9}$$

The velocities must be transformed to the individual omni-wheel slip frames to establish the slip

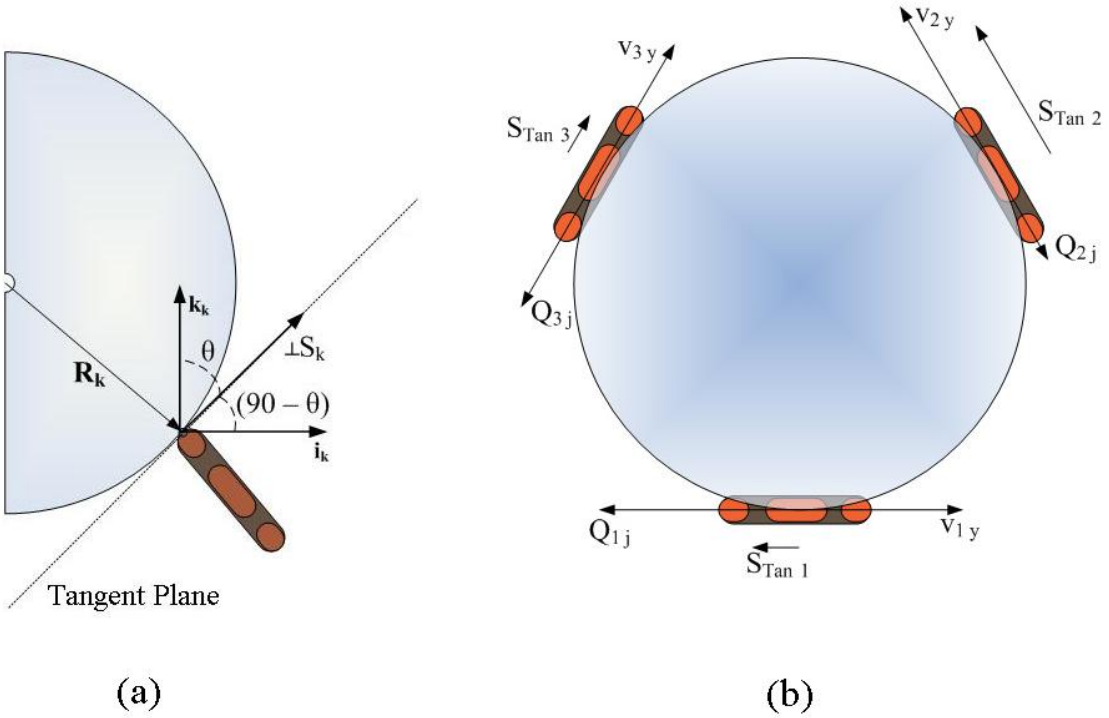

Figure 6: (a) Transverse velocity component and (b) tangential velocity component of slip.

transverse and tangential components:

$$\mathbf{Q}_k \quad = \quad \mathbf{T}_k^{-1}\mathbf{\Lambda}_k. \tag{10}$$

4.1 Tangential Slip Velocity Component

First, the tangential slip velocity, $S_{\tan_k}$, which is in the direction of the j-axis of frame $[i_k, j_k, k_k]$ shall be computed:

$$S_{\tan_k} \quad = \quad v_{k_y} - Q_{k_j}. \tag{11}$$

Note that both the y-axis and j-axis directions are the same, and hence may be added directly.

4.2 Slip Ratio

The tangential slip velocity $S_{\tan_k}$ has components due to both the omni-wheel (v_{ky}) and the Atlas sphere (Q_{k_j}). Since these two mating elements posses different velocities at the contact point, there will be a resulting slip ratio. The slip ratio, SR_k, or slip percentage, is a measure of how much faster $S_{\tan_k}$ is compared to the Atlas sphere Q_{k_j}:

$$SR_k = \left(\frac{S_{\tan_k}}{Q_{k_j}}\right) 100. \tag{12}$$

The slip ratio quantifies the slip between the Atlas sphere and the omni-wheel at a specific contact point in the tangential velocity direction. The sign of SR_k determines in what direction on

the j-axis (y-axis) the tangential slip velocity is pointing. If the absolute value of SR_k is greater than 100% then the tangential slip velocity is greater than the Atlas sphere's tangential velocity at that contact point. Conversely, if the absolute value of SR_k is below 100% then the Atlas sphere tangential velocity is greater $S_{\tan_k}$. If both the omni-wheel and the Atlas sphere tangential velocities were identical, then there would be no slip: we would have $S_{\tan_k} = 0$, and there would be no slip ratio. Alternately, if $Q_{k_j} \approx 0$, then Equation 12 tends towards infinity. Note that achieving tangential slip of zero is a control objective.

4.3 Transverse Slip Velocity

The transverse slip velocity, $S_{\perp_k}$, relies only on the Atlas sphere's velocity component in the tangent plane perpendicular to the tangential slip velocity, $S_{\tan_k}$. The omni-wheel does not contribute to the transverse slip velocity because there is no actuation of the omni-wheel in this direction; therefore the slip ratio is always unity since the free-spinning castor wheels will rotate at the same speed as the Atlas sphere in the transverse direction. From Equation (10) for each contact point and the tangential plane geometry:

$$S_{\perp_k} \quad = \quad Q_{k_i} \cos(90^\circ - \theta) + Q_{k_k} \cos\theta. \tag{13}$$

4.4 Slip Velocity Vector

The slip velocity at each contact point, expressed in the plane defined by $S_{\perp_k}$ and $S_{\tan_k}$ is simply the vector comprised of the two components:

$$\mathbf{S}_k \quad = \quad \begin{bmatrix} S_{\perp_k} \\ S_{\tan_k} \end{bmatrix}. \tag{14}$$

5 Examples

The following examples illustrate the levels of slip involved in actuating the Atlas sphere using omni-wheels as discussed above. Clearly, the largest control challenge is coping with the non-holonomic differential constraints arising from the slip induced by the actuation. Regarding trajectory generation there are two ways, conceptually, to deal with the non-integrable velocity constraints and estimate the pose of the sphere at any instant given a set of omni-wheel angular velocity inputs: either numerically integrate the angular velocity relations expressed by Equation (8) based on information embedded in the slip model; or integrate rate sensor output on the sphere to estimate pose. For Atlas sphere orientation control, some form of computed pose state is needed to be compared with the integrated sensed rate output.

5.1 Example 1

In this example omni-wheel 1 is given an angular velocity of 1 rad/s, while omni-wheels 2 and 3 remain stationary. The omni-wheel radius is $r_z = 0.1$ m, while the sphere radial vector components are $R_X = 0.75$ m, $R_Y = 0$ m, $R_Z = -0.25$ m. The computed angular velocity of the sphere is $\Omega_X = -0.04$ rad/s, $\Omega_Y = 0$ rad/s, $\Omega_Z = -0.12$ rad/s, with $\|\mathbf{\Omega}\| = 0.1265$ rad/s. The angular velocity vector of the sphere should generate slip at the contact points with the two fixed omni-wheels.

k	SR_k (%)	$S_{\tan_k}$ (m/s)	$S_{\perp_k}$ (m/s)
1	0	0	0
2	100	0.0850	-0.0274
3	100	0.0850	0.0274

Table 1: Slip for Example 1.

The output of the slip model is listed in Table 1. As may have been expected, there is no slip on the one rotating omni-wheel, but there is 100% slip on the two stationary wheels.

5.2 Example 2

In this example a pure *roll* rotation (about the X-axis) is generated. The omni-wheel inputs are $\omega_1 = 1$ rad/s, $\omega_2 = -0.5$ rad/s, and $\omega_3 = -0.5$ rad/s. Note: to generate pure *pitch* (about the Y-axis) we must have $\omega_1 = 0$, and $\omega_2 = -\omega_3$; to generate pure *yaw* (about the Z-axis) we must have $\omega_1 = \omega_2 = \omega_3$.

k	SR_k (%)	$S_{\tan_k}$ (m/s)	$S_{\perp_k}$ (m/s)
1	-566.6667	-0.0850	0
2	566.6667	0.0425	-0.0411
3	566.6667	0.0425	0.0411

Table 2: Slip for Example 2.

For omni-wheel and sphere geometry the same as in Example 1, the outputs are listed in Table 2. It is to be seen that the slip ratio for each omni-wheel is more than 500%. The major conclusion to be drawn from Examples 1 and 2 is that slip is a significant issue for state estimation for pose level kinematics.

6 Conclusions

The Atlas simulator motion platform employs three omni-directional wheels to provide changes in platform orientation. This actuation concept will typically produce slip between the omni-wheels and the Atlas sphere at the contact points. The slip-vectors lie on tangent planes of the Atlas sphere. The slip is modelled by three parameters: the tangential-slip velocity, $S_{\tan_k}$; the transverse-slip velocity, $S_{\perp_k}$; and the slip ratio, SR_k.

Given the non-holonomic velocity constraints of the actuation concept, no integrating factor exists permitting a solution of the associated differential equations. Thus, the orientation of the sphere at any given instant is impossible to determine given a set of omni-wheel angular velocity values. This was the motivation for developing a slip model for the Atlas sphere. This model will be developed and used, together with rate-sensor data, during sphere angular displacements, to control the angular displacement level kinematics of the sphere.

References

[1] S. Jonsson. "New AGV with Revolutionary Movement". *Proc.* 3^{rd} *Int. Conf. on Automated Guided Vehicles,* Stockholm, pages 135–144, 1985.

[2] F. Williams, E.R. Laithwaite, and G.F. Eastham. "Development and Design of Spherical Induction Motors". *Proc IEEE*, vol. 47:471–484, Dec. 1959.

[3] R.B. Roth and K.-M. Lee. "Design Optimization of a Three-Degree-of-Freedom Variable Reluctance Spherical Wrist Motor". *ASME J. Eng. Industry*, vol. 117:378–388, 1995.

[4] S. Toyama, S. Sugitani, G. Zhang, Y. Miyatani, and K Nakamura. "Multi Degree of Freedom Spherical Ultrasonic Motor". *Proc 1995 IEEE Int. Conf. Robotic and Automation*, pages 2935–2940, 1995.

[5] G.S. Chirikjian and D. Stein. "Kinematic Design and Commutation of a Spherical Stepper Motor". *IEEE/ASME Transactions on Mechatronics*, vol. 4, no. 4:342–353, 1999.

[6] J. Robinson, J.B. Holland, M.J.D. Hayes, and R.L. Langlois. "Velocity Level Control of a Spherical Orienting Device Using Omni-directional Wheels". Submitted to 2^{nd} *CCToMM Symposium on Machines, Mechanisms and Mechtronics,* Canadian Space Agency, May 26-27, 2005.

[7] R. Williams, D. Carter, P. Gallina, and G. Rosati. "Dynamics Model with Slip for Wheeled Omni-Directional Robots". *IEEE Transactions on Robotic and Automation*, vol. 18, no. 3:285–293, 2002.

[8] J. Angeles. *Fundamentals of Robotic Mechanical Systems: Theory, Methods, and Algorithms.* Springer-Verlag, New York, N.Y., U.S.A., 1997.